Bubble-stabilised polytopal scheme for flows in fractured media with frictional contact

Jérôme Droniou

from joint works with R. Masson, A. Haidar, G. Enchéry and I. Faille.

IMAG, CNRS & University of Montpellier, France,
School of Mathematics, Monash University, Australia

https://imag.umontpellier.fr/~droniou/

WCCM 2024 / PANACM 2024, 23 July 2024

Funded by the European Union

European Research Council
Established by the European Commission

References for this presentation

- Design of the method, application to poromechanics with Coulomb friction: [Droniou et al., 2024a].
- Analysis for purely mechanical model with Tresca friction: [Droniou et al., 2024b].

See also references inside.

Outline

Matrix and fracture network

Notations: Ω domain (matrix), Γ fracture, two sides $\pm$ with outward normals $\mathbf{n}^{\pm}$.

Uknowns: displacement $\mathbf{u}$ in matrix (discontinuous at fractures), pressure p_m in matrix, pressure p_f in fracture.

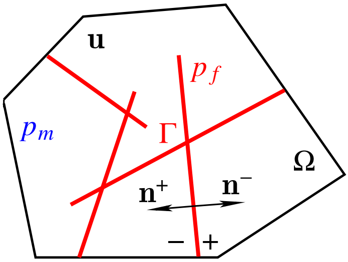

Poromechanics I

Flow equations: Darcy law for p_m, Poiseuille law for p_f.

$$\begin{cases} \partial_t \phi_m + \operatorname{div} \mathbf{V}_m = h_m & \text{on } (0,T)\times\Omega\backslash\overline{\Gamma}, \\ \mathbf{V}_m = -\frac{\mathbb{K}_m}{\eta}\nabla p_m & \text{on } (0,T)\times\Omega\backslash\overline{\Gamma}, \\ \partial_t \mathrm{d}_f + \operatorname{div}_{\boldsymbol{\tau}} \mathbf{V}_f - [\![\mathbf{V}_m]\!]_n = h_f & \text{on } (0,T)\times\Gamma, \\ \mathbf{V}_f = \frac{C_f}{\eta}\nabla_{\boldsymbol{\tau}} p_f, & \text{on } (0,T)\times\Gamma, \\ \gamma_{\mathbf{n}}^{\pm}\mathbf{V}_m = \Lambda_f [\![p]\!]^{\pm} & \text{on } (0,T)\times\Gamma. \end{cases}$$

Notations:

- $[\![\cdot]\!]$: jump across Γ.
- $\boldsymbol{X}_{\boldsymbol{\tau}}$ and $X_{\mathbf{n}}$: tangential and normal components of $\boldsymbol{X}$ along Γ.

Poromechanics II

Set

$$\begin{aligned}
&\sigma(\mathbf{u}) = 2\mu\varepsilon(\mathbf{u}) + \lambda(\operatorname{div}\mathbf{u})\ \mathbb{I} && \text{(Effective stress)},\\
&\sigma^\top(\mathbf{u}, p_m) = \sigma(\mathbf{u}) - b p_m\ \mathbb{I} && \text{(Total stress)},\\
&\mathbf{T}^\pm = \gamma_{\mathbf{n}}^\pm \sigma^\top(\mathbf{u}, p_m) + p_f \mathbf{n}^\pm && \text{(Traction)}.
\end{aligned}$$

Mechanical equations: quasi-static contact-mechanics for $\mathbf{u}$ with Coulomb friction.

$$\begin{cases}
-\operatorname{div}\sigma^\top(\mathbf{u}, p_m) = \mathbf{f} & \text{on } (0,T)\times\Omega\backslash\overline{\Gamma},\\
\mathbf{T}^+ + \mathbf{T}^- = 0 & \text{on } (0,T)\times\Gamma,\\
T_{\mathbf{n}} \leqslant 0,\ [\![\mathbf{u}]\!]_{\mathbf{n}} \leqslant 0,\ [\![\mathbf{u}]\!]_{\mathbf{n}} T_{\mathbf{n}} = 0, & \text{on } (0,T)\times\Gamma,\\
|\mathbf{T}_{\boldsymbol{\tau}}| \leqslant -F\ T_{\mathbf{n}} & \text{on } (0,T)\times\Gamma,\\
\mathbf{T}_{\boldsymbol{\tau}} \cdot \partial_t [\![\mathbf{u}]\!]_{\boldsymbol{\tau}} - F\ T_{\mathbf{n}}\, |\partial_t [\![\mathbf{u}]\!]_{\boldsymbol{\tau}}| = 0 & \text{on } (0,T)\times\Gamma
\end{cases}$$

Other contact models: no friction ($F = 0$); Tresca friction ($-FT_{\mathbf{n}} \rightsquigarrow g$ and $\partial_t[\![\mathbf{u}]\!] \rightsquigarrow [\![\mathbf{u}]\!]$.

Poromechanics III

Weak formulation for mechanical equations: using Lagrange multiplier $\boldsymbol{\lambda} = -\mathbf{T}^+$ to impose the contact conditions.

Spaces and cone:

$$\mathbf{U}_0 = \{\mathbf{v} \in H^1(\Omega\backslash\overline{\Gamma})^d \ : \ \mathbf{v}_{|\partial\Omega} = 0\},$$

$$\boldsymbol{C}_f(\lambda_\mathbf{n}) = \Big\{\boldsymbol{\mu} \in H^{-1/2}(\Gamma)^d \ : \ \langle \boldsymbol{\mu}, \mathbf{v}\rangle_\Gamma \le \langle F\lambda_\mathbf{n}, |\mathbf{v}_{\boldsymbol{\tau}}|\rangle_\Gamma \quad \forall \mathbf{v} \in (H^{1/2}(\Gamma))^d \text{ s.t. } v_\mathbf{n} \le 0\Big\}.$$

Equations: find $\mathbf{u} : [0,T] \to \mathbf{U}_0$ and $\boldsymbol{\lambda} : [0,T] \to \boldsymbol{C}_f(\lambda_n)$ s.t., for all $\mathbf{v} : [0,T] \to \mathbf{U}_0$ and $\boldsymbol{\mu} : [0,T] \to \boldsymbol{C}_f(\lambda_n)$,

$$\int_\Omega \Big(\sigma(\mathbf{u}) : \varepsilon(\mathbf{v}) - b \ p_m \mathrm{div}(\mathbf{v})\Big) + \langle \boldsymbol{\lambda}, [\![\mathbf{v}]\!]\rangle_\Gamma + \int_\Gamma p_f \ [\![\mathbf{v}]\!]_\mathbf{n} = \int_\Omega \mathbf{f} \cdot \mathbf{v},$$

$$\langle \mu_\mathbf{n} - \lambda_\mathbf{n}, [\![\mathbf{u}]\!]_\mathbf{n}\rangle_\Gamma + \langle \boldsymbol{\mu}_{\boldsymbol{\tau}} - \boldsymbol{\lambda}_{\boldsymbol{\tau}}, [\![\partial_t \mathbf{u}]\!]_{\boldsymbol{\tau}}\rangle_\Gamma \le 0.$$

Outline

Mesh

Polytopal mesh, compatible with fractures

- $\mathcal{M}, \mathcal{F}, \mathcal{V}$ cells, faces and vertices. $\mathcal{X}_{\mathrm{z}}$ entities $\mathcal{X}$ on z.
- $\mathcal{F}^{+}_{\Gamma,K}$ faces of K on positive side of fracture.
- For $s \in \mathcal{V}$, $\mathcal{K}s$: set of cells on the same side of K.
- If $\sigma \in \mathcal{F}_{\Gamma}$: K on positive side, L on negative side.

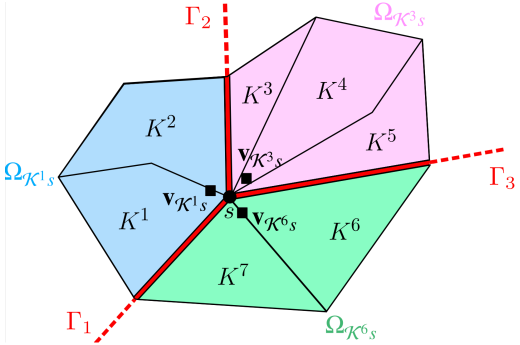

Discrete spaces

Displacement: nodal unknowns (discontinuous across fracture) and one bubble on each fracture face (positive side).

$$\mathbf{U}_{0,\mathcal{D}} = \Big\{ \mathbf{v}_{\mathcal{D}} = \big((\mathbf{v}_{\mathcal{K}s})_{K\in\mathcal{M},\, s\in\mathcal{V}_K}, (\mathbf{v}_{K\sigma})_{K\in\mathcal{M},\, \sigma\in\mathcal{F}^{+}_{\Gamma,K}} \big) \ : \\ \mathbf{v}_{\mathcal{K}s} \in \mathbb{R}^d,\ \mathbf{v}_{K\sigma} \in \mathbb{R}^d,\ \mathbf{v}_{\mathcal{K}s} = 0 \text{ if } s \in \mathcal{V}^{\text{ext}} \\ \mathbf{v}_{\mathcal{K}s} = \mathbf{v}_{\mathcal{L}s} \text{ if } K, L \text{ are on the same side of } \Gamma \Big\}.$$

Lagrange multipliers: piecewise constant on fracture faces.

$$\mathbf{M}_{\mathcal{D}} = \left\{ \boldsymbol{\lambda}_{\mathcal{D}} \in L^2(\Gamma)^d \ : \ \boldsymbol{\lambda}_{\sigma} := (\boldsymbol{\lambda}_{\mathcal{D}})_{|\sigma} \text{ is constant for all } \sigma \in \mathcal{F}_{\Gamma} \right\}.$$

Discrete dual cone:

$$\mathbf{C}_{\mathcal{D}} = \left\{ \boldsymbol{\lambda}_{\mathcal{D}} \in \mathbf{M}_{\mathcal{D}} \ : \ \lambda_{\mathcal{D},\mathbf{n}} \geq 0,\ |\boldsymbol{\lambda}_{\mathcal{D},\boldsymbol{\tau}}| \leq \mathrm{g} \right\} \subset \boldsymbol{C}_f.$$

Reconstructions in $\mathbf{U}_{0,\mathcal{D}}$: faces

- From nodes, reconstruct edge values and use them to define the face gradient:

$$\nabla^{K\sigma}\mathbf{v}_{\mathcal{D}} = \frac{1}{|\sigma|}\sum_{e=s_1s_2\in\mathcal{E}_\sigma}|e|\frac{\mathbf{v}_{\mathcal{K}s_1}+\mathbf{v}_{\mathcal{K}s_2}}{2}\otimes\mathbf{n}_{\sigma e}.$$

Reconstructions in $\mathbf{U}_{0,\mathcal{D}}$: faces

- From nodes, reconstruct edge values and use them to define the face gradient:

$$\nabla^{K\sigma}\mathbf{v}_{\mathcal{D}} = \frac{1}{|\sigma|}\sum_{e=s_1 s_2 \in \mathcal{E}_\sigma} |e| \frac{\mathbf{v}_{\mathcal{K}s_1} + \mathbf{v}_{\mathcal{K}s_2}}{2} \otimes \mathbf{n}_{\sigma e}.$$

- Reconstruct face averaged value from nodes, and face displacement:

$$\overline{\mathbf{v}}_{K\sigma} = \sum_{s \in \mathcal{V}_\sigma} \omega_s^\sigma \mathbf{v}_{\mathcal{K}s} \quad \text{and} \quad \Pi^{K\sigma}\mathbf{v}_{\mathcal{D}}(\mathbf{x}) = \nabla^{K\sigma}\mathbf{v}_{\mathcal{D}}(\mathbf{x} - \overline{\mathbf{x}}_\sigma) + \overline{\mathbf{v}}_{K\sigma} \quad \forall \mathbf{x} \in \sigma.$$

Reconstructions in $\mathbf{U}_{0,\mathcal{D}}$: faces

- From nodes, reconstruct edge values and use them to define the face gradient:

$$\nabla^{K\sigma}\mathbf{v}_{\mathcal{D}} = \frac{1}{|\sigma|}\sum_{e=s_1s_2\in\mathcal{E}_\sigma}|e|\frac{\mathbf{v}_{\mathcal{K}s_1}+\mathbf{v}_{\mathcal{K}s_2}}{2}\otimes\mathbf{n}_{\sigma e}.$$

- Reconstruct face averaged value from nodes, and face displacement:

$$\overline{\mathbf{v}}_{K\sigma} = \sum_{s\in\mathcal{V}_\sigma}\omega_s^\sigma\mathbf{v}_{\mathcal{K}s} \quad \text{and} \quad \Pi^{K\sigma}\mathbf{v}_{\mathcal{D}}(\mathbf{x}) = \nabla^{K\sigma}\mathbf{v}_{\mathcal{D}}(\mathbf{x}-\overline{\mathbf{x}}_\sigma)+\overline{\mathbf{v}}_{K\sigma} \quad \forall\mathbf{x}\in\sigma.$$

- Jump reconstructions:

$$[\![\mathbf{v}_{\mathcal{D}}]\!]_\sigma = \overline{\mathbf{v}}_{K\sigma}-\overline{\mathbf{v}}_{L\sigma}+\mathbf{v}_{K\sigma}.$$

Reconstructions in $\mathbf{U}_{0,\mathcal{D}}$: cells

Same principles...

- Using reconstructed face values and bubble, define the cell gradient:

$$\nabla^K \mathbf{v}_{\mathcal{D}} = \frac{1}{|K|} \sum_{\sigma \in \mathcal{F}_K} |\sigma| \overline{\mathbf{v}}_{K\sigma} \otimes \mathbf{n}_{K\sigma} + \frac{1}{|K|} \sum_{\sigma \in \mathcal{F}^+_{\Gamma,K}} |\sigma| \mathbf{v}_{K\sigma} \otimes \mathbf{n}_{K\sigma}.$$

Reconstructions in $\mathbf{U}_{0,\mathcal{D}}$: cells

Same principles...

- Using reconstructed face values and bubble, define the cell gradient:

$$\nabla^K \mathbf{v}_{\mathcal{D}} = \frac{1}{|K|} \sum_{\sigma \in \mathcal{F}_K} |\sigma| \overline{\mathbf{v}}_{K\sigma} \otimes \mathbf{n}_{K\sigma} + \frac{1}{|K|} \sum_{\sigma \in \mathcal{F}^+_{\Gamma,K}} |\sigma| \mathbf{v}_{K\sigma} \otimes \mathbf{n}_{K\sigma}.$$

- Reconstruct cell averaged value from nodes, and cell displacement:

$$\overline{\mathbf{v}}_K = \sum_{s \in \mathcal{V}_K} \omega_s^K \mathbf{v}_{\mathcal{K}s} \quad \text{and} \quad \Pi^K \mathbf{v}_{\mathcal{D}}(\mathbf{x}) = \nabla^K \mathbf{v}_{\mathcal{D}}(\mathbf{x} - \overline{\mathbf{x}}_K) + \overline{\mathbf{v}}_K \quad \forall \mathbf{x} \in K.$$

Reconstructions in $\mathbf{U}_{0,\mathcal{D}}$: cells

Same principles...

- Using reconstructed face values and bubble, define the cell gradient:

$$\nabla^K \mathbf{v}_{\mathcal{D}} = \frac{1}{|K|} \sum_{\sigma \in \mathcal{F}_K} |\sigma| \overline{\mathbf{v}}_{K\sigma} \otimes \mathbf{n}_{K\sigma} + \frac{1}{|K|} \sum_{\sigma \in \mathcal{F}_{\Gamma,K}^{+}} |\sigma| \mathbf{v}_{K\sigma} \otimes \mathbf{n}_{K\sigma}.$$

- Reconstruct cell averaged value from nodes, and cell displacement:

$$\overline{\mathbf{v}}_K = \sum_{s \in \mathcal{V}_K} \omega_s^K \mathbf{v}_{\mathcal{K}s} \quad \text{and} \quad \Pi^K \mathbf{v}_{\mathcal{D}}(\mathbf{x}) = \nabla^K \mathbf{v}_{\mathcal{D}}(\mathbf{x} - \overline{\mathbf{x}}_K) + \overline{\mathbf{v}}_K \quad \forall \mathbf{x} \in K.$$

Global reconstructions: $[\![\cdot]\!]_{\mathcal{D}}$, $\nabla^{\mathcal{D}}$, $\Pi_{\mathcal{D}}$, $\mathbb{e}_{\mathcal{D}}$, $\mathrm{div}_{\mathcal{D}}$, $\mathbb{\sigma}_{\mathcal{D}}$.

Scheme

Find $\mathbf{u}_{\mathcal{D}} \in \mathbf{U}_{0,\mathcal{D}}$ and $\boldsymbol{\lambda}_{\mathcal{D}} \in \mathbf{M}_{\mathcal{D}}$ s.t.

$$\int_{\Omega} \sigma_{\mathcal{D}}(\mathbf{u}_{\mathcal{D}}) : \varepsilon_{\mathcal{D}}(\mathbf{v}_{\mathcal{D}}) + \sum_{K \in \mathcal{M}} (2\mu_K + \lambda_K) S_K(\mathbf{u}_{\mathcal{D}}, \mathbf{v}_D) + \int_{\Gamma} \boldsymbol{\lambda}_{\mathcal{D}} \cdot [\![\mathbf{v}_{\mathcal{D}}]\!]_{\mathcal{D}} = \int_{\Omega} \mathbf{f} \cdot \Pi^{\mathcal{D}} \mathbf{v}_{\mathcal{D}} \qquad \forall \mathbf{v}_{\mathcal{D}} \in \mathbf{U}_{0,\mathcal{D}}$$

$$\int_{\Gamma} (\boldsymbol{\mu}_{\mathcal{D}} - \boldsymbol{\lambda}_{\mathcal{D}}) \cdot [\![\mathbf{u}_{\mathcal{D}}]\!]_{\mathcal{D}} \leq 0 \qquad \forall \boldsymbol{\mu}_{\mathcal{D}} \in \mathbf{M}_{\mathcal{D}},$$

where

$$S_K(\mathbf{u}_{\mathcal{D}}, \mathbf{v}_{\mathcal{D}}) = h_K^{d-2} \sum_{s \in \mathcal{V}_K} \left(\mathbf{u}_{\mathcal{K}s} - \Pi^K \mathbf{u}_{\mathcal{D}}(\mathbf{x}_s) \right) \cdot \left(\mathbf{v}_{\mathcal{K}s} - \Pi^K \mathbf{v}_{\mathcal{D}}(\mathbf{x}_s) \right) + h_K^{d-2} \sum_{\sigma \in \mathcal{F}^+_{\Gamma,K}} \mathbf{u}_{K\sigma} \cdot \mathbf{v}_{K\sigma}.$$

Note: can also be written in virtual elements framework.

Outline

Error estimate

Theorem (Error estimate)

If $\mathbf{u} \in H^2(\mathcal{M})$ *and* $\boldsymbol{\lambda} \in H^1(\mathcal{F}_\Gamma)$*, then*

$$\|\nabla^{\mathcal{D}}\mathbf{u}_{\mathcal{D}} - \nabla\mathbf{u}\|_{L^2(\Omega\setminus\overline{\Gamma})} + \|\boldsymbol{\lambda}_{\mathcal{D}} - \boldsymbol{\lambda}\|_{-1/2,\Gamma} \lesssim C_{\mathbf{u},\boldsymbol{\lambda}} h_{\mathcal{D}}.$$

- $\|\cdot\|_{-1/2,\Gamma}$ discrete $H^{-1/2}$-like seminorm.
- Error estimate comes from a more abstract version that only requires $\boldsymbol{\lambda} \in L^2(\Gamma)$.
- Error analysis based on consistency and stability.

Tool 1: discrete Korn inequality

Discrete H^1-norm:

$$\|\mathbf{v}_\mathcal{D}\|_{1,\mathcal{D}}^2 := \sum_{K\in\mathcal{M}} \left(\|\nabla^K \mathbf{v}_\mathcal{D}\|_{L^2(K)}^2 + S_K(\mathbf{v}_\mathcal{D}, \mathbf{v}_\mathcal{D}) \right).$$

Theorem (Discrete Korn inequality)

For all $\mathbf{v} \in \mathbf{U}_{0,\mathcal{D}}$,

$$\|\mathbf{v}_\mathcal{D}\|_{1,\mathcal{D}}^2 \lesssim \|\mathbb{e}_\mathcal{D}(\mathbf{v}_\mathcal{D})\|_{L^2(\Omega\setminus\overline{\Gamma})}^2 + \sum_{K\in\mathcal{M}} S_K(\mathbf{v}_\mathcal{D}, \mathbf{v}_\mathcal{D}).$$

Tool 2: Discrete inf–sup property I

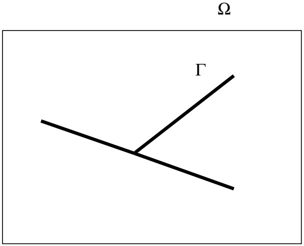

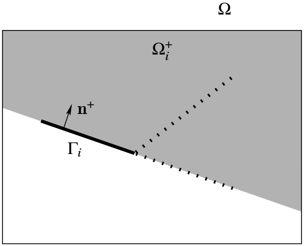

Definition (Discrete $H^{-1/2}(\Gamma)$-norm)

For $\boldsymbol{\lambda}_\mathcal{D} \in \mathbf{M}_\mathcal{D}$:

$$\|\boldsymbol{\lambda}_\mathcal{D}\|_{-1/2,\Gamma} = \sum_{i\in I} \|\boldsymbol{\lambda}_\mathcal{D}\|_{-1/2,\Gamma_i} \quad \text{with} \quad \|\boldsymbol{\lambda}_\mathcal{D}\|_{-1/2,\Gamma_i} = \sup_{\mathbf{v}_i \in H^1(\Omega_i^+;\Gamma_i)^d \setminus\{0\}} \frac{\int_{\Gamma_i} \boldsymbol{\lambda}_\mathcal{D} \cdot \mathbf{v}_i}{\|\mathbf{v}_i\|_{H^1(\Omega_i^+)}}.$$

Tool 2: Discrete inf–sup property II

Theorem (Discrete inf-sup condition)

$$\sup_{\mathbf{v}_\mathcal{D}\in\mathbf{U}_{0,\mathcal{D}}\setminus\{0\}} \frac{\int_\Gamma \boldsymbol{\lambda}_\mathcal{D}\cdot[\![\mathbf{v}_\mathcal{D}]\!]_\mathcal{D}}{\|\mathbf{v}_\mathcal{D}\|_{1,\mathcal{D}}} \gtrsim \|\boldsymbol{\lambda}_\mathcal{D}\|_{-1/2,\Gamma} \qquad \forall\boldsymbol{\lambda}_\mathcal{D}\in\mathbf{M}_\mathcal{D}.$$

- *Ingredient 1*: Clément-like H^1-stable interpolator adapted to fractures.
- *Ingredient 2*: Fortin property for jump: for $\mathbf{v}_i \in H^1(\Omega_i^+;\Gamma_i)$ and $\mathbf{v}_\mathcal{D}$ = interpolant of extension by 0 of $\mathbf{v}_i$ by 0,

$$\int_\Gamma \boldsymbol{\lambda}_\mathcal{D}\cdot[\![\mathbf{v}_\mathcal{D}]\!]_\mathcal{D} = \int_{\Gamma_i} \boldsymbol{\lambda}_\mathcal{D}\cdot\mathbf{v}_i.$$

Outline

Outline

2D domain with fracture under compression I

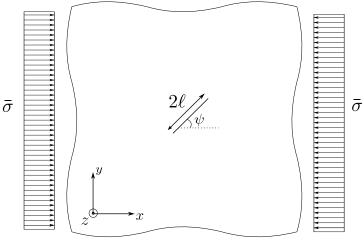

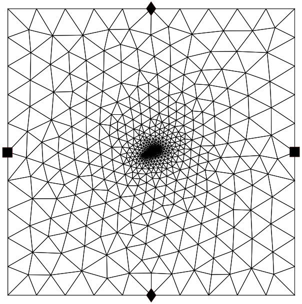

Analytical solution (τ coordinate along fracture):

$$\lambda_{\mathbf{n}} = \sigma \sin^2(\psi),$$

$$|[\![\mathbf{u}]\!]_{\boldsymbol{\tau}}| = \frac{4(1-\nu)}{E} \sigma \sin(\psi) \left(\cos(\psi) - \frac{\mathsf{g}}{\lambda_{\mathbf{n}}} \sin(\psi) \right) \sqrt{\ell^2 - (\ell^2 - \tau^2)}.$$

$\psi = \pi/9$, $2\ell = 2$ m, $F = 1/\sqrt{3}$ (so $\mathsf{g} = \lambda_{\mathbf{n}}/F$), $E = 25$ GPa and $\nu = 0.25$.

2D domain with fracture under compression II

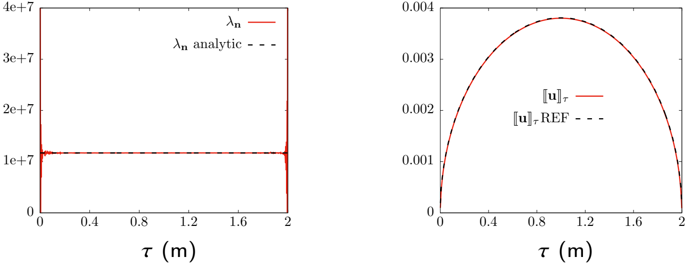

2D domain with fracture under compression III

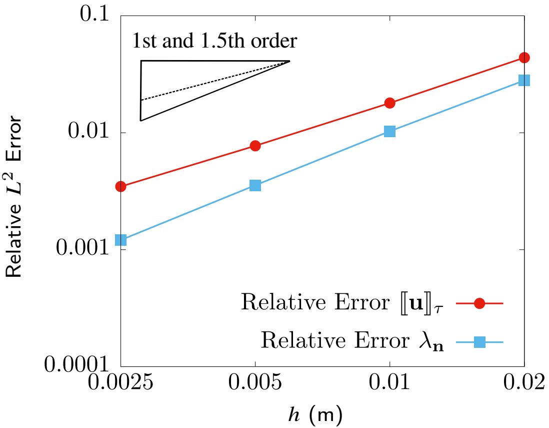

Note: error on $\lambda_\mathbf{n}$ away from the tip, super-convergence due to the fact that the analytic $\boldsymbol{\lambda}$ is constant.

3D manufactured solution I

Setting:

- $\Omega = (-1,1)^3$, $\Gamma = \{0\} \times (-1,1)^2$.
- $g = 1$, $\mu = \lambda = 1$.
- Explicit analytical solution such that:
  - sticky-contact for $z < 0$ ($[\![u]\!]_{\mathbf{n}} = 0$, $[\![u]\!]_{\boldsymbol{\tau}} = 0$)
  - slippy-contact for $z > 0$ ($[\![u]\!]_{\mathbf{n}} = 0$, $|[\![u]\!]_{\boldsymbol{\tau}}| > 0$)
- Cartesian, tetrahedral and generalised hexahedral meshes.

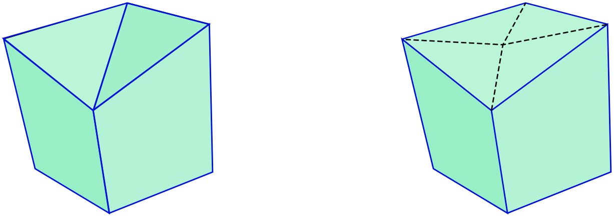

Figure: Generalised hexahedral meshes: cut (left) and barycentric subdivisions (right).

3D manufactured solution II

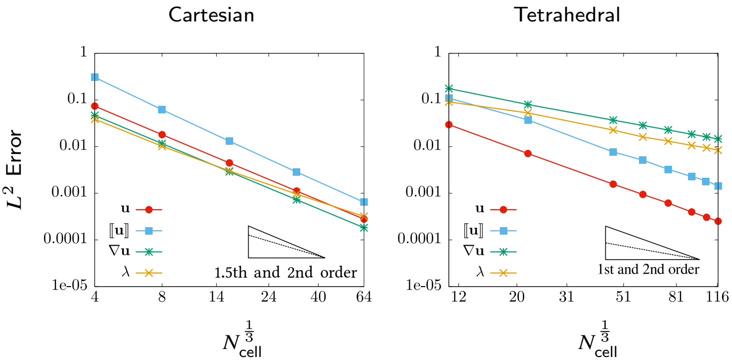

Note: 10^{-2} accuracy for $\mathbf{u}$ achieved with $\sim 40^3$ Cartesian cells, $\sim 60^3$ triangular cells.

3D manufactured solution III

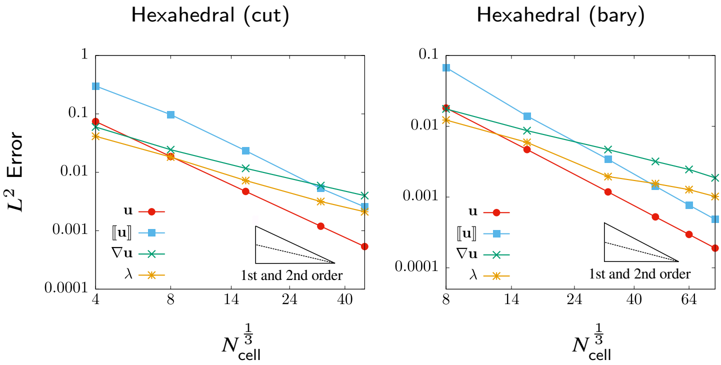

Note: 10^{-2} accuracy for $\mathbf{u}$ achieved with $\sim 30^3$ Hexahedral cells.

Outline

Setting

Data: $E = 4$Gpa, $\nu = 0.2$, $F = 0.5$, $b = 0.5$, $M = 10$GPa.

Dirichlet BC at the top and bottom for $\mathbf{u}$.

Fracture network:

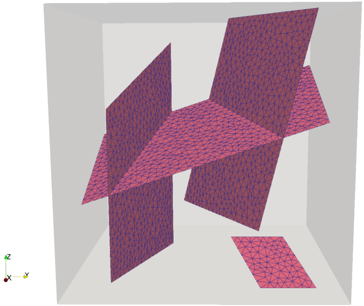

Two tetrahedral meshes: 47k and 127k elements.

Results I

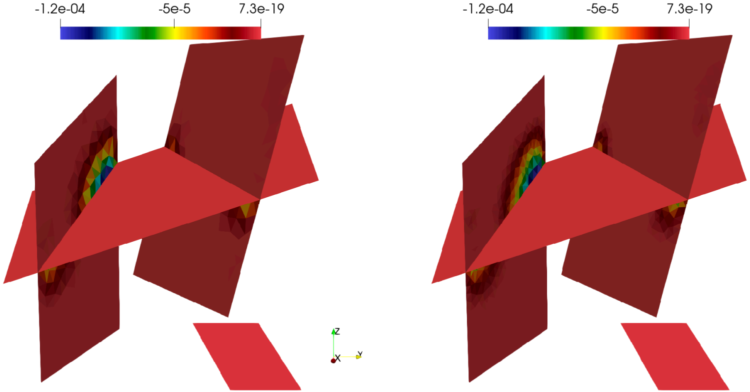

Figure: Normal displacement jumps using 47k cells (left) and 127k cells (right).

Results II

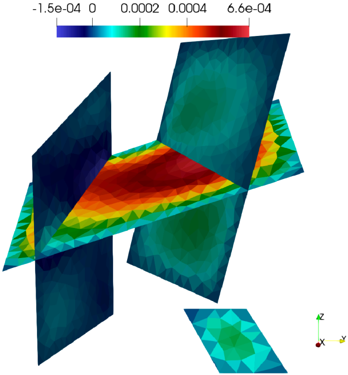

Figure: Tangential displacement jumps (one direction) using 47k cells (left) and 127k cells (right).

Conclusions

- Polytopal scheme, applicable on generic meshes (including hanging nodes, cut cells, local refinements). Seamlessly handles crossing fractures, etc.
- Bubble enrichment (first one for polytopal methods) to ensure inf-sup conditions to bound Lagrange multipliers.
- Complete analysis for mechanical models.
- Robust simulations (including solver behaviour) for 3D poromechanical model with network of fractures.
- Ongoing work: extension to arbitrary order of approximation, analysis for complete poromechanical model.

Funded by
the European Union

European Research Council
Established by the European Commission

Funded by the European Union (ERC Synergy, NEMESIS, project number 101115663). Views and opinions expressed are however those of the authors only and do not necessarily reflect those of the European Union or the European Research Council Executive Agency. Neither the European Union nor the granting authority can be held responsible for them.

Thank you for your attention!

References I

Droniou, J., Enchéry, G., Faille, I., Haidar, A., and Masson, R. (2024a).
A bubble vem–fully discrete polytopal scheme for mixed-dimensional poromechanics with frictional contact at matrix-fracture interfaces.
Computer Methods in Applied Mechanics and Engineering, 422:116838.
https://arxiv.org/abs/2312.09319.

Droniou, J., Haidar, A., and Masson, R. (2024b).
Analysis of a vem–fully discrete polytopal scheme with bubble stabilisation for contact mechanics with tresca friction.
page 34p.
Submitted, http://arxiv.org/abs/2404.03045.